

The Discovery of an Ultra-Faint Star Cluster in the Constellation of Ursa Minor¹

R. R. Muñoz^{2,3}, M. Geha², P. Côté⁴, L. C. Vargas², F. A. Santana³, P. Stetson⁴, J. D. Simon⁵ & S. G. Djorgovski^{6,7}

ABSTRACT

We report the discovery of a new ultra-faint globular cluster in the constellation of Ursa Minor, based on stellar photometry from the MegaCam imager at the Canada-France-Hawaii Telescope (CFHT). We find that this cluster, Muñoz 1, is located at a distance of 45 ± 5 kpc and at a projected distance of only $45'$ from the center of the Ursa Minor dSph galaxy. Using a Maximum Likelihood technique we measure a half-light radius of $0'.5$, or equivalently 7 pc and an ellipticity consistent with being zero. We estimate its absolute magnitude to be $M_V = -0.4 \pm 0.9$, which corresponds to $L_V = 120^{+160}_{-65} L_\odot$ and we measure a heliocentric radial velocity of -137 ± 4 km s⁻¹ based on Keck/DEIMOS spectroscopy. This new satellite is separate from Ursa Minor by ~ 30 kpc and 110 km s⁻¹ suggesting the cluster is not obviously associated with the dSph, despite the very close angular separation. Based on its photometric properties and structural parameters we conclude that Muñoz 1 is a new ultra-faint stellar cluster. Along with Segue 3 this is one of the faintest stellar clusters known to date.

¹Based on observations obtained at the Canada-France-Hawaii Telescope (CFHT) which is operated by the National Research Council of Canada, the Institut National des Sciences de l'Univers of the Centre National de la Recherche Scientifique of France, and the University of Hawaii. Spectroscopic data presented herein were obtained at the W. M. Keck Observatory, which is operated as a scientific partnership among the California Institute of Technology, the University of California and the National Aeronautics and Space Administration.

²Astronomy Department, Yale University, New Haven, CT 06520, USA

³Departamento de Astronomía, Universidad de Chile, Camino El Observatorio 1515, Las Condes, Santiago, Chile (rmunoz@das.uchile.cl)

⁴Herzberg Institute of Astrophysics, National Research Council of Canada, Victoria, BC, V9E 2E7, Canada

⁵Observatories of the Carnegie Institution of Washington, 813 Santa Barbara St., Pasadena, CA 91101, USA

⁶Astronomy Department, California Institute of Technology, Pasadena, CA, 91125, USA

⁷Distinguished Visiting Professor, King Abdulaziz University, Jeddah, Saudi Arabia.

Subject headings: galaxies: photometry - globular clusters: general - Galaxy: halo - Local Group

1. Introduction

Over the last seven years, and thanks to the advent of the Sloan Digital Sky Survey (SDSS; York et al. 2000), seventeen new Milky Way satellites have been discovered (e.g., Willman et al. 2005; Zucker et al. 2006a,b; Belokurov et al. 2006, 2007; Irwin et al. 2007). The majority of these objects correspond to a new class of ultra low-luminosity dwarf galaxies, based on their kinematic and metallicity properties (e.g., Muñoz et al. 2006; Martin et al. 2007; Simon & Geha 2007), with luminosities ranging from $M_V \sim -8$ for the brighter of these objects down to an extreme $M_V \sim -1.5$ for the faintest (Martin et al. 2008). Given their extremely low stellar contents, they are commonly referred to as the Ultra-Faint Dwarfs (UFDs). A few other systems are clearly low luminosity globular clusters, which include Koposov 1 and 2 ($M_V = -1$ and -2 respectively; Koposov et al. 2007) and the extreme case of Segue 3 ($M_V \sim 0.0$; Belokurov et al. 2010; Fadelly et al. 2011).

Despite the enormous success of satellites searches in SDSS, this survey covers only about a fourth of the sky down to a magnitude limit of $r \sim 22.5$. In practice this means that the faintest objects can only be detected out to distances smaller than a few tens of kiloparsecs (see Fig. 9 in Tollerud et al. 2008), and thus the majority of the Milky Way’s virial volume remains unsearched for UFDs and other faint stellar systems.

In this Letter we present the discovery of a new extremely low-luminosity, outer halo stellar cluster, in the outskirts of the Ursa Minor dwarf spheroidal (dSph) galaxy. This discovery was made just outside the SDSS footprint using significantly deeper photometry which allowed us to probe farther into the Milky Way halo. In §2 we detail the data-set and the discovery. In §3 we present the results from the photometric analysis and in §4 we show radial velocity data recently obtained. Finally, in §5 we discuss and summarize our results.

2. Data and Discovery

The discovery of this new system was made serendipitously while analyzing photometric data for the Ursa Minor dSph galaxy taken with the MegaCam imager at the Canada-France-Hawaii Telescope (CFHT). MegaCam is a wide-field imager consisting of 36 2048×4612 pixel CCDs, covering almost a full 1×1 deg² field of view with a pixel scale of $0''.187$ pixel⁻¹. These data were taken as part of a larger program aimed at obtaining deep wide-field imaging of

all bound stellar over-densities in the Milky Way halo beyond 25 kpc (R. R. Muñoz et al. 2012, in preparation). Ursa Minor was observed on the nights of UT June 12-14 and July 07-13, 2010 under dark conditions with typical seeing of $0.7 - 0''.9$. Four different, slightly overlapping fields were observed for a total area coverage of nearly $2 \times 2 \text{ deg}^2$. In each field, the center of the dSph was placed in one of the corners so that, when combined, the galaxy is located at the center of the covered area. We obtained six dithered exposures of 360 seconds in both the g - and r -band. A standard dithering pattern was used to cover both small and large gaps present between the chips.

MegaCam images are delivered to the user pre-processed by the CFHT team using the “Elixir” package (Magnier & Cuillandre 2004). Subsequent photometric measurements were carried out using first DAOPHOT/Allstar, and later running the ALLFRAME package on the processed frames, following the procedure outlined in Stetson (1994). Finally, astrometric solutions were calculated using the freely available SCAMP¹ code, and photometric calibration was carried out by direct comparison with data from the SDSS-Data Release 7 (DR7; Abazajian & Sloan Digital Sky Survey 2009). For more details on the method see Muñoz et al. (2010).

As seen in Figure 1 and the left panel of Figure 2, we discovered a centrally concentrated over-density of stars $45'$ to the south-west of Ursa Minor. Based on the structural parameters determined below, we presume this object to be an ultra-faint globular cluster and therefore name it Muñoz 1. In §5 we discuss in more depth our reasoning for this classification. Figure 2 also shows the color-magnitude diagram (CMD) of the central region of Muñoz 1 where a distinct main-sequence turn-off is observed. Assuming the stars in the red-giant branch (RGB) region are members of the cluster we fit an isochrone at a distance of 45 kpc, an age of 12.5 Gyr and $[\text{Fe}/\text{H}] = -1.5$. We note that this fit is very tentative given the very low number of stars that belong to the system. The right panel of the figure compares the CMDs of UMi and the new object showing a clear difference in distance modulus.

3. Structural Properties

We carry out a maximum-likelihood analysis of the photometric data for Muñoz 1 following the method of Martin et al. (2008) as described in Muñoz et al. (2010). This method starts by assuming a shape for the underlying light distribution; in this case we have tried three of the most commonly used profiles for UFDs, a King (King 1962), exponential and Plummer (Plummer 1911) density laws. We then fit simultaneously the structural

¹See <http://www.astromatic.net/software/scamp>.

parameters of the object, i.e., scale length (half-light radius or King core and tidal radii depending on the profile), coordinates of the center of the cluster, ellipticity, position angle and background density. To estimate parameter uncertainties we carry out a bootstrap analysis of 10000 realizations of the photometric data.

Table 1 shows the resulting parameters. We obtain a half-light radius of 7.1 ± 2.1 pc using both an exponential and Plummer profile, whereas a King profile yields $r_{\text{core}} = 4.5 \pm 1.9$ pc and $r_{\text{tidal}} = 65 \pm 28$ pc.

Figure 3 shows the number density profile for Muñoz 1. We have overplotted the three best-fit profiles, all of which give a reasonable description of the light distribution. The right panel of this figure shows a density contour map of the object, where the contours represent 2, 3, 5, 8, 12 and 18 – σ levels above the background density. These contours show no evident elongation or tidal features. Applying a bootstrap analysis where we generate 10000 realizations of the photometric data (Walsh et al. 2008; Muñoz et al. 2010), we determine that the asymmetries observed in the outer parts, toward the south and west directions, are not statistically significant due to the very low number of stars.

In addition to the structural parameters, we estimate the absolute magnitude of the new object. We follow the method described in Muñoz et al. (2010) which relies in the total number of stars that belong to the cluster and not on the sum of their fluxes. As shown by Martin et al. (2008) the low number of stars identified in the ultra-faint systems, especially true in the case of Muñoz 1, makes traditional methods of adding the individual fluxes of the member stars very sensitive to the inclusion (or exclusion) of potential members, especially at brighter magnitudes. To alleviate shot noise issues we use an alternative method based on a model stellar population. For this we use a theoretical luminosity function that best describes the photometric properties of the cluster, in this case a 12.5 Gyr old population with $[\text{Fe}/\text{H}] = -1.5$ (Dotter et al. 2008). We then integrate the LF to obtain the total flux down to a given magnitude limit. The last step is to scale this flux using the total number of stars that belong to the cluster down to the same magnitude limit. We estimate the corresponding uncertainty through a bootstrap analysis. This yields $M_V = -0.4 \pm 0.9$ mag assuming a Chabrier initial mass function (Chabrier 2001), which corresponds to $L_V = 120^{+160}_{-65} L_{\odot}$. Only one old star cluster has a published luminosity lower than Muñoz 1, the Segue 3 stellar cluster with a total luminosity of $M_V = -0.0 \pm 0.8$ mag (Fadely et al. 2011), although given the large uncertainties in both measurements it is unclear which cluster is actually fainter.

4. Spectroscopic Properties

Spectroscopic data of photometrically selected Muñoz 1 candidate stars were taken on UT May 28, 2011 with the Keck II 10-m telescope and the DEIMOS spectrograph (Faber et al. 2003). One Keck/DEIMOS multi-slit mask was observed with the 1200 line mm^{-1} grating covering a wavelength region $6400 - 9100\text{\AA}$ with a spectral dispersion of 0.33\AA . The mask was observed for 7800 seconds under relatively poor seeing conditions which varied between $1.5 - 2''$. Spectra were reduced using a modified version of the spec2d software pipeline (version 1.1.4) developed by the DEEP2 team, and radial velocities were determined using the software described by Simon & Geha (2007). For additional details, we refer the reader to Geha et al. (2009).

Radial velocities were successfully measured for 24 of the 47 extracted spectra. Stars for which we could not measure a velocity were primarily very low S/N spectra of faint objects near the expected main sequence turn-off of Muñoz 1 ($r \sim 22 - 22.5$).

The resulting velocity distribution is shown in Figure 4, along with the corresponding spatial and color-magnitude distributions. While the velocity histogram does not show a clear significant peak that could be interpreted as the velocity signature of Muñoz 1, if we restrict ourselves to the most centrally concentrated stars, what appears as a cold peak is indeed discerned. Using the four stars closest to the derived center of the cluster, plus a fifth star possibly associated with it based on its radial velocity, distance to the cluster and position in the CMD, we estimate a mean velocity of $-137 \pm 4 \text{ km s}^{-1}$. Given the small number of stars and large velocity uncertainties, we estimate only a one sigma upper limit on the velocity dispersion of $\sigma < 4.7 \text{ km s}^{-1}$. Given the size and luminosity of Muñoz 1, we predict its velocity dispersion to be between $0.2 - 0.3 \text{ km s}^{-1}$ based on Wolf et al. (2010) and a mass-to-light ratio consistent with old stars only. Our measured velocity dispersion is consistent with this value, but we cannot rule out a scenario where the mass of Muñoz 1 is significantly larger than its stellar mass.

Two other stars with radial velocities in the vicinity of this peak do not live near the CMD of Muñoz 1, nor are they close to the center of the object, and therefore we consider them less likely to be associated with the cluster. We also observe three stars consistent with the published radial velocity of Ursa Minor of -245 km s^{-1} (Muñoz et al. 2005). These stars are less spatially concentrated than the Muñoz 1 stars and yield a mean velocity of $-253 \pm 6 \text{ km s}^{-1}$, in good agreement with the observed value for the dSph galaxy.

A subset of stars in our Keck/DEIMOS kinematic sample have sufficient S/N (at least 10\AA^{-1}) to determine their metallicities. We determine $[\text{Fe}/\text{H}]$ based on fitting synthetic spectra, as described in Kirby et al. (2008). This medium-resolution technique allows us

to calculate T_{eff} and $[\text{Fe}/\text{H}]$ by matching an observed Keck/DEIMOS spectrum to a grid of models with different T_{eff} and $[\text{Fe}/\text{H}]$. This is in contrast to most high resolution abundances, which are based on equivalent widths and require resolved, unblended lines. Our spectral resolution is not sufficient for such type of analysis. We note, however, that our well-characterized noise array enables us to calculate realistic error bars.

We measure metallicities for two stars kinematically associated with Ursa Minor and one star associated with Muñoz 1. The two Ursa Minor stars have metallicities $[\text{Fe}/\text{H}] = -2.78 \pm 0.60$ and -2.30 ± 0.68 , while the Muñoz 1 star has $[\text{Fe}/\text{H}] = -1.46 \pm 0.32$. These results are consistent with the isochrone-derived metallicity. Due to the paucity of Fe II absorption lines in cool RGB spectra, we are unable to calculate surface gravity from the spectroscopic data. Hence, to estimate $[\text{Fe}/\text{H}]$ we had to fix $\log g$ from the best-fit isochrone. The code also outputs a value for T_{eff} , which can be compared to the value obtained using the de-reddened CFHT photometry. For the case of the cluster star, we obtain a $T_{\text{eff}} = 5160 \pm 320$ K, in good agreement with the photometric value of $T_{\text{eff}} = 5290$ K.

5. Summary and Discussion

We report the discovery of a new ultra-faint stellar system, Muñoz 1, in the Ursa Minor constellation, located only $45'$ from the center of the Ursa Minor dSph. The discovery was made serendipitously while analyzing photometric data for Ursa Minor, taken with the wide-field MegaCam imager on the CFHT. We visually fit a 12.5 Gyr isochrone from the Dartmouth database (Dotter et al. 2008), with a metallicity of $[\text{Fe}/\text{H}] = -1.5$ at a distance of ~ 45 kpc. While the close angular distance between these two Galactic satellites might suggest an association, we deem it unlikely. We have estimated the escape velocity from Ursa Minor at the projected distance of Muñoz 1, i.e., 1 kpc, assuming the dSph is a point mass of $1 \times 10^8 M_{\odot}$ (Wolf et al. 2010). We obtain $v_{\text{esc}} \sim 30$ km s $^{-1}$, much smaller than the ~ 110 km s $^{-1}$ of radial velocity difference. Moreover, at 30 kpc, the distance separating the cluster from the dSph along the line of sight, v_{esc} decreases down to only a few km s $^{-1}$.

Using a maximum-likelihood technique, following the method of Martin et al. (2008), we have simultaneously derived structural parameters along with background density for Muñoz 1. Assuming different density profiles we have derived consistent half light radii of $r_{h, \text{exp}} = 7.1 \pm 2.8$ pc, $r_{h, P} = 7.1 \pm 2.1$ pc for exponential and Plummer profiles respectively, and a King core and tidal radii of $r_c = 4.5 \pm 1.9$ and $r_t = 65 \pm 28$ pc respectively. The total luminosity of Muñoz 1, on the other hand, was derived using the method described in Muñoz et al. (2010), which relies in the total number of stars in the object instead of their individual fluxes, obtaining an absolute magnitude of $M_V = -0.4 \pm 0.9$, equivalent to $L_V =$

$120_{-65}^{+160} L_{\odot}$. Based on its photometric properties, we argue that this new Galactic satellite corresponds to an extremely faint globular cluster. Since the discovery of the UFDs, there has been some debate in the literature about the classification of stellar over-densities based solely on photometric information. It has been argued, for instance, that objects like Segue 1 and Coma Berenices should be considered large globular clusters based on the assumption that galaxies cannot have scale lengths smaller than ~ 100 pc (Gilmore et al. 2007). On the other hand, spectroscopic information, i.e., velocity dispersions and metallicities, have been used to argue that despite their sizes, these systems correspond to dark matter dominated galaxies (Simon & Geha 2007; Geha et al. 2009). For Muñoz 1, the spectroscopic information is insufficient to determine unambiguously whether the object is dark matter dominated or not. However, this satellite is significantly smaller than any of the known dwarf galaxies, including the UFDs, it lies within the size distribution of other Milky Way globular clusters with structural parameters similar to other outer halo clusters like Palomar 13 (Bradford et al. 2011), and while in principle it could be the smallest known galaxy, without a reliable measurement of its velocity dispersion or metallicity spread, we view it as much more likely that it is a globular cluster. The luminosity derived for this object, makes it one of the faintest globular cluster discovered, only nominally surpassed by Segue 3, which has an absolute magnitude of $M_V = 0.0 \pm 0.8$ (Fadely et al. 2011). Given the large uncertainties of both measurements, it is unclear which one of them is indeed fainter. The density profile of this object is well fitted by typical cluster density profiles showing no obvious hints for significant tidal disruption.

The discovery of this cluster was made in the context of a larger program aimed at obtaining deep and wide-field photometry for all outer halo satellites regardless of morphological classification. At the time of this publication, we have imaged roughly 40 deg^2 down to a magnitude limit of $r \sim 24.5 - 25$ depending on the object. As pointed out by Tollerud et al. (2008), surveys deeper than SDSS are bound to uncover fainter and more distant ultra-faint systems. Naively extrapolating the discovery of at least one ultra-faint cluster in our surveyed area to the entire sky, yields potentially a thousand similar objects still uncovered. While this number is not intended as a firm prediction given its large uncertainty, it foreshadows a much more complex picture of the globular cluster system in the outer halo than we have today.

We thank the referee for useful comments that helped improve this paper. We acknowledge Robert Zinn for useful discussions. This work was supported in part by the facilities and staff of the Yale University Faculty of Arts and Sciences High Performance Computing Center. R.R.M. acknowledges support from the GEMINI-CONICYT Fund, allocated to the project N°32080010, from CONICYT through project BASAL PFB-06 and the Fondo Nacional de Investigación Científica y Tecnológica (Fondecyt project N°1120013).

M. G. acknowledges support from the National Science Foundation under award number AST-0908752 and the Alfred P. Sloan Foundation. S.G.D. acknowledges partial support from the NSF grant AST-0909182.

REFERENCES

- Abazajian K., Sloan Digital Sky Survey f. t., 2009, ApJS, 182, 543
- Belokurov V., et al., 2006, ApJ, 647, L111
- Belokurov V., et al., 2007, ApJ, 654, 897
- Belokurov V., Walker M. G., Evans N. W., Gilmore G., Irwin M. J., Just D., Koposov S., Mateo M., Olszewski E., Watkins L., Wyrzykowski L., 2010, ApJ, 712, L103
- Bradford J. D., Geha M., Muñoz R. R., Santana F. A., Simon J. D., Côté P., Stetson P. B., Kirby E., Djorgovski S. G., 2011, ApJ, 743, 167
- Chabrier G., 2001, ApJ, 554, 1274
- Dotter A., Chaboyer B., Jevremović D., Kostov V., Baron E., Ferguson J. W., 2008, ApJS, 178, 89
- Faber S. M., et al., 2003, in Instrument Design and Performance for Optical/Infrared Ground-based Telescopes. Edited by Iye & Moorwood, Proceedings of the SPIE, Volume 4841, pp. 1657 The DEIMOS spectrograph for the Keck II Telescope: integration and testing
- Fadely R., Willman B., Geha M., Walsh S., Muñoz R. R., Jerjen H., Vargas L. C., Da Costa G. S., 2011, AJ, 142, 88
- Geha M., Willman B., Simon J. D., Strigari L. E., Kirby E. N., Law D. R., Strader J., 2009, ApJ, 692, 1464
- Gilmore G., Wilkinson M. I., Wyse R. F. G., Kleyna J. T., Koch A., Evans N. W., Grebel E. K., 2007, ApJ, 663, 948
- Irwin M., et al., 2007, ApJ, 656, L13
- King I., 1962, AJ, 67, 471
- Kirby E. N., Guhathakurta P., Sneden C., 2008, ApJ, 682, 1217

- Koposov S., de Jong J. T. A., Belokurov V., Rix H.-W., Zucker D. B., Evans N. W., Gilmore G., Irwin M. J., Bell E. F., 2007, *ApJ*, 669, 337
- Magnier E. A., Cuillandre J.-C., 2004, *PASP*, 116, 449
- Martin N. F., de Jong J. T. A., Rix H.-W., 2008, *ApJ*, 684, 1075
- Martin N. F., Ibata R. A., Chapman S. C., Irwin M., Lewis G. F., 2007, *MNRAS*, 380, 281
- Muñoz R. R., Carlin J. L., Frinchaboy P. M., Nidever D. L., Majewski S. R., Patterson R. J., 2006, *ApJ*, 650, L51
- Muñoz R. R., Frinchaboy P. M., Majewski S. R., Kuhn J. R., Chou M.-Y., Palma C., Sohn S. T., Patterson R. J., Siegel M. H., 2005, *ApJ*, 631, L137
- Muñoz R. R., Geha M., Willman B., 2010, *AJ*, 140, 138
- Plummer H. C., 1911, *MNRAS*, 71, 460
- Schlegel D. J., Finkbeiner D. P., Davis M., 1998, *ApJ*, 500, 525
- Simon J. D., Geha M., 2007, *ApJ*, 670, 313
- Stetson P. B., 1994, *PASP*, 106, 250
- Tollerud E. J., Bullock J. S., Strigari L. E., Willman B., 2008, *ApJ*, 688, 277
- Walsh S. M., Willman B., Sand D., Harris J., Seth A., Zaritsky D., Jerjen H., 2008, *ApJ*, 688, 245
- Willman B., et al., 2005, *ApJ*, 626, L85
- Wolf J., Martinez G. D., Bullock J. S., Kaplinghat M., Geha M., Muñoz R. R., Simon J. D., Avedo F. F., 2010, *MNRAS*, 406, 1220
- York D., et al., 2000, *AJ*, 120, 1579
- Zucker D. B., et al., 2006a, *ApJ*, 650, L41
- Zucker D. B., et al., 2006b, *ApJ*, 643, L103

Table 1. Parameters of Muñoz 1

Parameter	Mean	Uncertainty
$\alpha_{0,exp}$ (h m s)	15:01:48.02	$\pm 13''$
$\delta_{0,exp}$ (d m s)	+66:58:07.3	$\pm 8''$
$r_{h,exp}$ (arcmin)	0.49	± 0.19
$r_{h,exp}$ (pc)	7.1	± 2.8
$r_{h,P}$ (arcmin)	0.49	± 0.15
$r_{h,P}$ (pc)	7.1	± 2.1
r_c (arcmin)	15''	$\pm 9''$
r_c (pc)	4.5	± 1.9
r_t (arcmin)	3.6	± 2.2
r_t (pc)	65	± 28
M_V (Chabrier)	−0.4	± 0.9
L_V (L_\odot)	120	+160, −65
$\mu_{0,V}$ (mag arcsec $^{-2}$)	26.3	+1.6, −2.1
v_r (km s $^{-1}$)	−137	± 4
d (kpc)	45	± 5

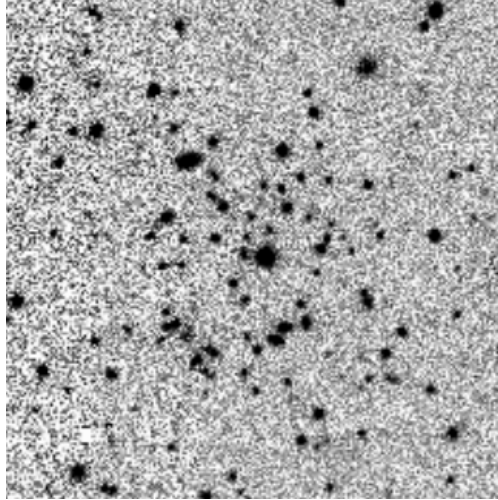


Fig. 1.— $1'.2 \times 1'.2$, r -band view of Muñoz 1. The image is roughly centered on the cluster. North is up, east is to the left.

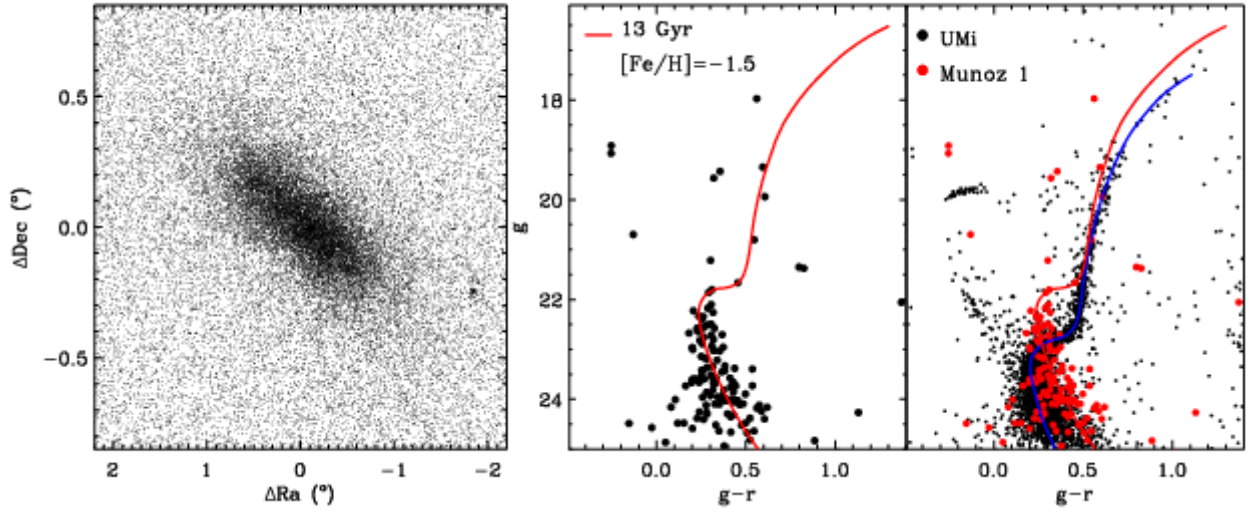


Fig. 2.— *left*: Star count map of the Ursa Minor dSph field. The primary object in this field is the dSph galaxy. Muñoz 1 lies $45'$ away from the center of the field in the south-west direction, near $(-1.8^\circ, -0.25^\circ)$. *middle*: g vs $g-r$ CMD of stars in the Muñoz 1 region (within $2'$ of the measured center). The best fit isochrone is overplotted, corresponding to a Dartmouth (Dotter et al. 2008), 12.5 Gyr, $[\text{Fe}/\text{H}] = -1.5$ at a distance of ~ 45 kpc using a reddening value of $E(g-r) = 0.027$, adopted from the Schlegel et al. (1998) maps. *right*: CMD of Ursa Minor stars (small black points) overplotted on Muñoz 1 stars (large red symbols). Red and blue solid lines represent best fit isochrones for both the Ursa Minor dSph and Muñoz 1 respectively.

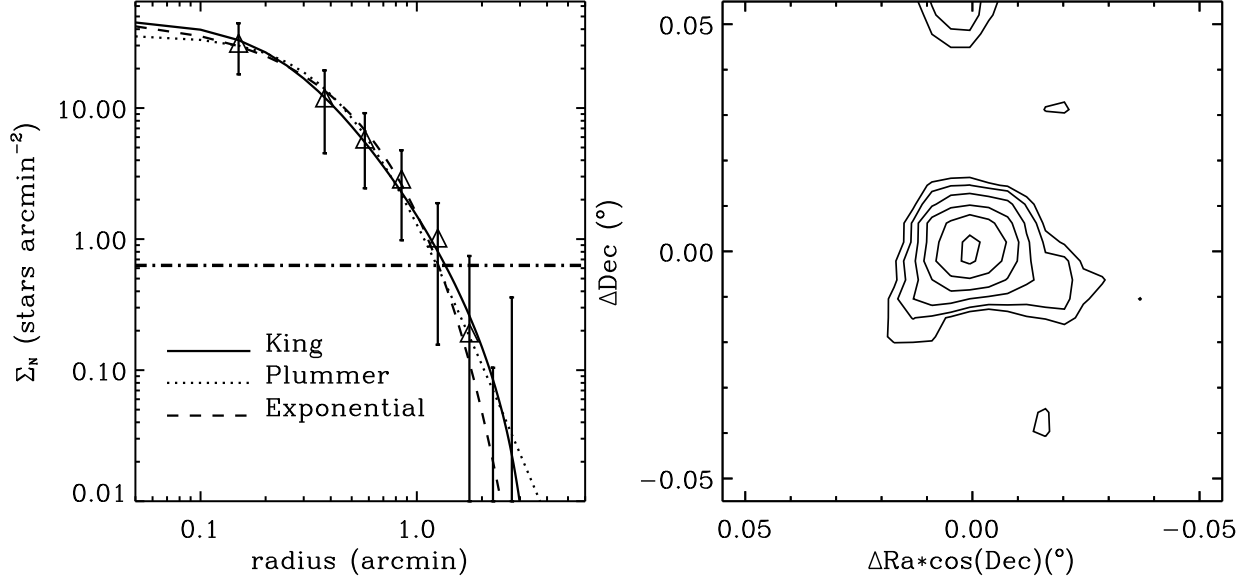


Fig. 3.— *Left*: Number density profile for Muñoz 1. Plummer, King and exponential profiles have been fitted to the data using a maximum likelihood method. The dot-dashed line represents the measured background density. *Right*: Iso-density contours for Muñoz 1. Contours level correspond to 2,3,5,8,12 and 18- σ level over the background density.

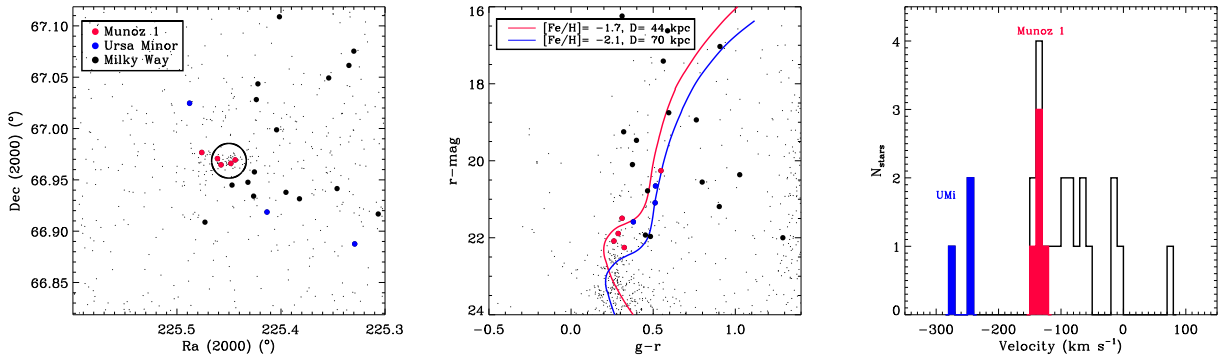


Fig. 4.— Keck/DEIMOS spectroscopic coverage of Muñoz 1, showing the spatial distribution (*left*), color-magnitude diagram (*middle*) and velocity distribution of targets (*right*). Red symbols in each panel indicate stars possibly associated with Muñoz 1, while blue symbols are stars likely associated with Ursa Minor.